Summer Project Report

Predicting neutron star observables from proposed equations of state

Arjun Murlidhar

August 2021

Abstract

A number of proposed modern equations of state of the interior of a neutron star are used to construct neutron star models and predict observables such as mass-radius relation and moment of inertia. This is done by numerically solving the Tolman–Oppenheimer–Volkoff (TOV) equation for each equation of state.

Using current observational data and the results obtained, we are able to eliminate some EoS models and constrain the possible dense matter equation of state.

Acknowledgements

I would like to sincerely thank my project supervisor Professor Dipankar Bhattacharya (IUCAA), for guiding me through this project and giving me his valuable time. I would like to thank my institute, IISER Pune, for giving me an oppurtunity to do this project.

Contents

1 Theory of Neutron Stars **4**
- 1.1 Introduction . . . 4
- 1.2 A brief history of neutron stars . . . 4
- 1.3 EoS of a cold degenerate ideal gas . . . 5
- 1.4 Towards a realistic equation of state - The HW EoS . . . 6
- 1.5 BPS-BBP equation of state . . . 7
- 1.6 Exotic states near the center? . . . 8
- 1.7 Equations of structure - The TOV equation . . . 8

2 Methodology **10**
- 2.1 The Objective . . . 10
- 2.2 Solving the TOV equation . . . 10
  - 2.2.1 Primer on numerical ODE solving - The Euler method . . . 10
  - 2.2.2 Details about the routine used . . . 11
- 2.3 Equations of state used in the project . . . 12

3 Results and discussion **13**
- 3.1 A simple example - degenerate ideal neutron gas . . . 13
- 3.2 Realistic Equations of state - AP3 . . . 16
- 3.3 Comparing Equations of state . . . 18
- 3.4 Conclusion . . . 20

1

Theory of Neutron Stars

1.1 Introduction

One of the biggest unsolved problems in astrophysics today is finding the exact equation of state of a neutron star. This has proved to be a difficult problem because our theoretical understanding of condensed matter at very high densities is incomplete and we cannot recreate such conditions in the laboratory either. Yet, over the past few decades, several equations of state of the interior of a neutron star have been proposed. We can use these equations of state to create models of neutron stars and predict astrophysical observables like masses, radii and moments of inertia.

As we gather more data from observations of neutron star masses and radii, we can eliminate some of these equations of state and place constraints on the state of matter at very high densities. Neutron stars can thus act as cosmic laboratories to test our theories of nuclear physics!

The advent of gravitational wave astronomy and the ability to detect neutron star mergers will allow us to observe more neutron stars that are not necessarily pulsars. Observing tiny deviations in the waveforms of binary neutron star inspirals due to tidal effects can place constraints on the stiffness of the equation of state.
Upgraded LIGO detectors, in the next couple of decades, will also be able to detect gravitational waves emitted during the last few cycles of inspiral of neutron stars and the ringdown of the remnant which carry crucial signatures of the properties of the dense matter equation of state.

The future of neutron star physics is exciting! But for now, let us take a few steps back to look at what we know and how we got here.

1.2 A brief history of neutron stars

In 1934, Baade and Zwicky proposed the idea of an ultra dense star composed only of neutrons. They made the remarkably prescient suggestion that neutron stars could be formed

in supernova explosions at the end of lives of massive stars.
The first calculation of neutron star models was done by Oppenheimer and Volkoff [5], who assumed a neutron star to be composed of an ideal gas of degenerate neutrons at 0 K (more about this in coming sections). Harrison, Wheeler and several others proposed improvements to this EoS.

Up till this time, the neutron star was a purely theoretical object and most physicists and astronomers did not believe in its existence. This changed with the discovery of the first pulsar by Jocelyn Bell and Antony Hewish in 1967. The leading theory to explain pulsars (which is generally accepted today) was that the pulses were created by spinning neutron stars.
Since 1968, there has been much theoretical work on the EoS of a neutron star. This was further stimulated by several discoveries of neutron stars in binary systems, beginning with the first "X-Ray Pulsar" in 1971. These are believed to be neutron stars in binary systems accreting gas from their normal companion stars and thereby emitting X-rays. This was followed by the discovery of the first binary pulsar by Hulse and Taylor (1975). Tracking the orbit of this binary system of a pulsar and a neutron star allowed for the first reliable mass measurement of a neutron star as well as a test of GR. Advancement in X-ray telescopes allowed us to estimate the radii of neutron stars by measuring thermal flux from the surface of low mass X-ray binaries.

Today, we know over 250 pulsars located in binary systems. We know the masses for $\sim$70 NS's and we have determined the radii of more than a dozen to be in the 9-13 km range [6].

1.3 EoS of a cold degenerate ideal gas

The first approximation to describing matter in a neutron star is to assume it to be a non interacting gas of neutrons at 0 K. A neutron star is not actually at 0 K. Newly born neutron stars cool to temperatures $< 10^9$ K within a few days and remain in the vicinity of $\sim 10^6$ K for at least 10,000 years. But this temperature is much smaller than typical energies associated with NS matter. For example, the excitation energy of nuclei $\sim 10^{10}$ K and Fermi energy (to be defined soon) $\sim 10^{12}$ K. Thus a neutron star can be very well approximated to be at 0 K.

A neutron is a Fermion and hence obeys the Fermi-Dirac statistics and Pauli's exclusion principle. Any quantum state (which corresponds to a single cell of side 'h' in momentum space, for free particles) can at most be occupied by two neutrons, both of opposite spin. Hence even at 0 K, there is a non zero maximum momentum of neutrons. This maximum momentum (magnitude) of neutrons is called Fermi momentum (p_F) and the corresponding energy is called Fermi energy (E_F).

All momentum states inside a sphere of radius p_F in momentum space will be occupied at absolute zero. Each momentum state is a cube of side h and each cube will have two particles. Number density of neutrons is given by the sum of particles over all momentum

states. Therefore,

$$n = 2 \cdot \frac{4\pi p_F^3/3}{h^3}$$

Hence, $p_F \propto n^{\frac{1}{3}}$. The relativistic expression for energy, $E = (p_F^2c^2 + m_o^2c^4)^{\frac{1}{2}}$ and the ideal gas expression for pressure are used along with the Fermi Dirac distribution function to find expressions for pressure and mass-energy density in terms of n(refer to [3]). The equation of state can then be derived from this. In the limit of non relativistic particles, $P \propto \rho^{\frac{5}{3}}$ and in the limit of ultra relativistic particles (i.e. v$\sim$c) $P \propto \rho^{\frac{4}{3}}$

1.4 Towards a realistic equation of state - The HW EoS

The most important assumption in constructing neutron star equations of state is that the NS matter has had enough time to come to thermal equilibrium and it is in the lowest energy state possible. The latter is a good assumption since NS's cool quickly to low temperatures and hence have to be in the ground state of matter (ref section 1.3).

The lowest energy configuration for a neutral gas of nucleons at zero pressure (i.e near the surface) is if the nucleons are arranged into $^{56}_{26}$Fe nuclei, since they have the lowest binding energy. Further these Fe atoms are arranged in a periodic lattice to minimise lattice energy. The equation of state for this state of matter until a density of $10^4 gcm^{-3}$ is well known and is called the Feynman-Metropolis-Teller EoS. At $10^4 gcm^{-3}$, atoms will get completely ionised and most of the pressure in this regime up till $10^7 gcm^{-3}$ is provided by the degenerate electron gas, whose EoS we discussed in section 1.3.

At higher densities, an important correction to the EoS is due to the inverse β decay reaction:

$$e^- + p \rightarrow n + \nu$$

This reaction can occur only if the fermi energy of the degenerate electrons exceeds the mass difference between the proton and neutron, $(m_p - m_n)c^2 = 1.29MeV$. The β decay reaction,

$$n \rightarrow p + e^- + \bar{\nu}$$

is the reverse reaction. In a neutron star, we can find the relative number of electrons, protons and neutrons by assuming equilibrium under β decay and imposing charge neutrality. The condition for equilibrium is,

$$\mu_e + \mu_p = \mu_n$$

where μ_i is the chemical potential and is equal to Fermi energy at 0 K. Using this equation and setting p_F of neutrons to be zero, we can find the mass density when neutrons first appear. This turns out to be $\sim 10^7 gcm^{-3}$.

For $\rho \geq 10^7 gcm^{-3}$, the electrons, now relativistically degenerate, begin to combine with protons in the iron-56 nuclei to produce more neutron rich nuclei. As $\frac{n_n}{n_p}$ increases, the effect of coulomb repulsion within the nucleus also decreases and the nuclei tend to get bigger. When the density increases to $\sim 4 \times 10^{11} gcm^{-3}$, the ratio $\frac{n_n}{n_p}$ reaches a critical value and any further increase in density causes the neutrons to "drip" out of the nuclei to form a sea of free neutrons along with free electrons and nuclei.

Harrison and Wheeler, in 1958, derived an equation of state for $\rho \geq 10^7\, g\, cm^{-3}$. They considered the total energy density of a system of free electrons, neutrons and nuclei,

$$\epsilon = n_N M(A,Z) + \epsilon_e(n_e) + \epsilon_n(n_n)$$

where M(A,Z) is the energy of nucleus (A,Z) and ϵ_n is the energy density of free neutrons. This is minimised w.r.t A, Z and n_n while keeping total baryon density constant. The quantity M(A,Z) for very neutron rich nuclei was inferred theoretically by Harrison and Wheeler using a *semi-empirical mass formula*. They made the approximation of treating A and Z as continuous variables.

Thus, for any A, one can find pressure and energy density of the degenerate electrons and if neutron drip is reached, that of degenerate free neutrons also.

$$\rho = \epsilon/c^2$$
$$P = P_e + P_n$$

P_i is the ideal degenerate gas pressure expression.

They found that neutron drip occurs at $\rho{\sim}3.18 \times 10^{11}\, g\, cm^{-3}$. Below this density, the pressure is provided by relativistically degenerate electrons and as the density increases above neutron drip, more neutrons begin to drip out and a greater fraction of the total pressure is provided by the free neutrons.

As density increases to $\rho \sim 4.54 \times 10^{12} g cm^{-3}$, almost 60% of the pressure is provided by neutrons. HW use the ideal degenerate gas EoS after this.

1.5 BPS-BBP equation of state

The HW EoS uses a fairly simplified function M(A,Z). But, real nuclei have discrete values of A and Z and shell effects play an important role in determining energy of the nucleus. Baym, Pethick and Suntherland proposed a modification to HW equation of state below neutron drip by using a better semi empirical formula extrapolated from laboratory nuclear energies. They also realised that *lattice energy* was important in determining equilibrium composition since it reduces the coulomb repulsive energy of the nucleus. BPS predicts the onset of neutron drip to be at $\rho \simeq 4.3 \times 10^{11}\, g\, cm^{-3}$.

Above neutron drip, there are two regimes. The first is the intermediate density regime with ρ between ρ_{drip} and the nuclear density $\rho_{nuc} = 2.8 \times 10^{14}\, g\, cm^{-3}$. At ρ_{nuc}, matter is packed so densely that nuclei begin to merge together and dissolve. This regime is fairly well understood. In the high density regime above ρ_{nuc}, the properties of matter are still uncertain. Our understanding of condensed matter at such high densities is incomplete. Neither do we know the correct form of the nuclear potential for interactions between nucleons, nor do we have a satisfactory many body computational method for solving the schrodinger equation.

The equation of state in the first regime was given by Baym, Bethe and Pethick in 1971. The BBP equation of state uses a mass formula which includes results from many body computations in it. The BPS EoS is smoothly matched to the BBP EoS at ρ_{drip}. The

adiabatic index γ till this point is $\simeq \frac{4}{3}$ corresponding to a relativistically degenerate electron gas.

γ drops steeply after this since the low density neutron gas that appears does not contribute much to pressure but it does to mass density. BBP find that nuclear saturation density occurs at $\rho_{nuc} = 2.4 \times 10^{14}\, g\, cm^{-3}$. At this point the nuclei are touching each other and at any higher density they dissolve to give liquid nuclear matter.

1.6 Exotic states near the center?

At densities higher than the nuclear density, there are speculations about some exotic phenomenon that might occur.

Firstly, a number of exotic particles might stably exist in the cores of neutron stars. When nucleons have high enough Fermi energies they might decay into their baryonic cousins hyperons in an inverse beta decay-like reaction.

In the beta decay reaction itself, if the neutrons have a large enough energy, they can decay into protons and pi mesons or K mesons instead of electrons (these are much heavier than electrons). Pi mesons are *bosons* as opposed to neutrons, protons and electrons which are fermions. At temperatures close to 0, a gas of bosons can undergo a phase transition to a *Bose-Einstein condensate* where all the particles occupy the lowest energy state. The pressure of such a gas is hence zero or very close to zero. Whether or not pions will form and pion condensation happens is still uncertain.

It has also been conjectured that there will be a hadron to quark phase transition at densities $\sim (5-10) \times \rho_{nuc}$ in a phenomenon called quark deconfinement. Equations of state that consider stars composed entirely of quarks have also been proposed.

Very shortly after the superconductivity was explained by the BCS theory, it was proposed that the liquid interior of a neutron star must have superconducting protons and superfluid neutrons. This has many observational consequences and can explain some observed behaviour of pulsars.

1.7 Equations of structure - The TOV equation

The final piece of the puzzle of modelling a neutron star is the Tolman-Oppenheimer-Volkoff equation. This is the general relativistic analog of the equation of hydrostatic equilibrium used in ordinary stars. Oppenheimer and Volkoff realised that for objects as dense as neutron stars, curvature of space will be significant and corrections due to GR cannot be neglected. This statement will be supported in the coming chapters by some of the results that have been obtained in this project.

To find the equations of neutron star structure, we need to find the metric of a neutron star. For this, we approximate a (non rotating) neutron star to be a static, spherically symmetric, perfect fluid. The most general spherically symmetric metric is given by,

$$ds^2 = -e^{2\Phi(r)}dt^2 + e^{2\Lambda(r)}dr^2 + r^2 d\Omega^2 \tag{1.1}$$

The stress energy tensor for a perfect fluid is,

$$T^{\mu\nu} = (\rho + p)u^{\mu}u^{\nu} + pg^{\mu\nu} \tag{1.2}$$

where $\mathbf{u}$ is the four velocity of the fluid. Since the star is assumed to be static in the coordinates we have used, the fluid's 3-velocity should be zero. Hence the normalised four velocity is given by $\mathbf{u} = (e^{-\Phi(r)}, 0, 0, 0)$ in (t, r, θ, ϕ) coordinates. p(r) and $\rho(r)$ are the isotropic pressure and density respectively.

By evaluating the four conservation equations, $\nabla \cdot \mathbf{T} = 0$, we get one non-trivial equation,

$$(\rho + p)\, \partial_r \Phi = -\partial_r p \tag{1.3}$$

To get the other equations of structure, we need to evaluate Einstein's field equations. The 00 component of the field equations, $G_{00} = 8\pi T_{00}$ gives,

$$\frac{d}{dr}[r\,(1 - e^{-2\Lambda})] = 8\pi r^2 \rho(r) \tag{1.4}$$

Let us denote $r\,(1 - e^{-2\Lambda})$ as $2m(r)$. Then, Eq 1.4 can be written as,

$$\frac{d}{dr}m(r) = 4\pi r^2 \rho(r) \tag{1.5}$$

It turns out, as we had anticipated, $m(r)$ has the interpretation of *total mass-energy inside radius r*. By evaluating the rr component of the field equations, we get,

$$\frac{d}{dr}\Phi(r) = \frac{m(r) + 4\pi r^3 p(r)}{r\,(r - 2m(r))} \tag{1.6}$$

Substituting Eq 1.3 in Eq 1.6 and putting the G's and c's back, we get the *TOV equation*,

$$\boxed{\frac{d}{dr}p(r) = \frac{-G\,(\rho(r)c^2 + p(r))(m(r)c^2 + 4\pi r^3 p(r))}{r\,(r - 2Gm(r)/c^2)}} \tag{1.7}$$

Equations 1.7 and 1.5 together with the equation of state can be used to find the structure of neutron stars.

2

Methodology

2.1 The Objective

As discussed in the previous chapter, the equation of state for densities smaller than the nuclear saturation density is fairly well understood. The uncertainty lies in densities above ρ_{nuc}. There have been several different calculations of EoS's in this regime that have been proposed, using methods like extrapolation from laboratory data, relativistic mean field theory and QCD calculations. Astrophysical observables of a neutron star such as mass, radius and moment of inertia depend sensitively on the equation of state above nuclear saturation. Stiffer (larger adiabatic index γ) EoS's lead to larger radii for a given mass and a larger maximum mass of neutron stars, whereas softer (smaller γ) EoS's predict a smaller maximum mass.

The objective of this project is to use these different equations of state and numerically solve the TOV equation to predict mass-radius relations and moment of inertia. Then compare these plots with observational data to constrain the possible nuclear equations of state.

2.2 Solving the TOV equation

Equations 1.7 and 1.5 form a set of coupled linear ordinary differential equations. Given the dependence of p on ρ, we can, in theory, integrate these equations to find p(r), $\rho(r)$ and m(r) for a given central density or pressure. But not only is the TOV equation difficult to solve analytically, most of the time, we don't have a functional form for the equation of state. Hence, the best course of action is to numerically solve this set of coupled ODE's.

2.2.1 Primer on numerical ODE solving - The Euler method

The general form of a system of N coupled linear ODE's is,

$$\frac{d}{dx}y_i = f_i\left(x, y_0, ..., y_{N-1}\right) \quad i = 0, .., N-1 \tag{2.1}$$

Given a set of initial conditions $(x^o, y_0^o, .., y_{N-1}^o)$, the Euler method determines the solution

using the recursive formula,

$$y_i^{n+1} = y_i^n + hf(x^n, y_0^n, .., y_{N-1}^n) \quad i = 0, .., N-1 \tag{2.2}$$

where $y_i^{n+1} = y_i(x_{n+1})$ and $x_{n+1} = x_n + h$. 'h' is called the step size.

The Euler method approximates the function at x_{n+1} as a Taylor expansion around x_n upto the linear term. Higher order methods such as the Runge-Kutta methods approximate the function up to higher order terms in the expansion without explicitly calculating all the derivatives. For example, the second order Runge-Kutta method for one variable:

$$k_1 = hf(x_n, y_n)$$
$$k_2 = hf(x_n + \frac{1}{2}h, y_n + \frac{1}{2}k_1)$$
$$y_{n+1} = y_n + k_2 + O(h^3)$$

Taylor expanding k_2 and keeping terms only up to second order will give the Taylor expansion for y_{n+1} correct up to second order .

2.2.2 Details about the routine used

For this project I used the Dormand-Prince fifth order Runge-Kutta method with adaptive step size control based on the code in *Numerical Recipes 3rd ed* [7].

The integration starts at a particular value of central pressure (initial value of p) at a radius, $r_0 = 1cm$. We can't start at exactly $r_0 = 0$ since the differential equations diverge at the center. The value of m_0 is calculated by assuming the density of the neutron star is constant from the center till r_0 and is equal to the central density. 1 cm is about six orders of magnitude smaller than the radius of a typical neutron star. Since we won't be considering results of the integration up to that precision, this is a good approximation to make.

The code from Numerical Recipes has been modified to stop when the pressure falls below a certain value. Ideally, we need to integrate the TOV equation until the pressure falls to zero since at the surface of the star there is no pressure. But neutron stars have a very thin solid crust made of crystalline $^{56}_{26}Fe$ which has a density of $10^6\, g\, cm^{-3}$. After this point, density falls to zero very rapidly (in less than a metre). Since this part of the star is not adding much to the mass or radius of the star up to the precision with which we are concerned, the integration is stopped at a pressure corresponding to a density of $\sim 10^4\, g\, cm^{-3}$.

Adaptive step size control used in this routine keeps track of the truncation error at each step and if this error is smaller than a given tolerance, then it scales up the step size. Otherwise, the step size is reduced. This was a very important feature to have in this project because of the large ranges of values involved. By using larger step sizes when the function is changing slowly and smaller steps otherwise, we can achieve the desired accuracy with as few steps as possible. In this project I've used a tolerance of about one part in 10^8.

In this routine, we can either obtain the values of functions p(r) and m(r) at regular intervals of a given size or at the points where the program lands during integration. Dense output at regular intervals is calculated by interpolating between the integration steps.

Mass-Radius relations can be calculated by running this integration for a range of central density values. Moment of inertia can be calculated by adding the MoI integral as a third differential equation to be simultaneously solved. Density profile of the neutron star was calculated by plotting the values of $\rho(r)$ at the integration steps.

2.3 Equations of state used in the project

The data for neutron star EoS is available in the form of tabulated values of pressure and the corresponding density. In order to find the value of p for any ρ or the other way around, we need to interpolate between the tabulated values. In this project, I've used the *cubic spline interpolation* routine from [7]. The cubic spline method uses the values of two tabulated points to find the value of any point in between in such a way that the first and second derivatives of the function are continuous in the interval and at the endpoints.

The list of equations of state used are as follows:
1. **Ideal degenerate gas of neutrons**: The relativistically correct expression for pressure and density as a function of $x_F = \frac{p_F}{m_o c}$ for a cold ideal gas in [3] was used to create a table of values of pressure vs density.
2. **ap3, ap4**: A. Akmal, V. R. Pandharipande, Phys. Rev. C 58, 1804 (1998)
3. **alf1**: M. Alford, M. Braby, M. Paris, and S. Reddy, Astrophys.J. 629, 969 (2005)
4. **ms1, ms2**: H. Muller and B. D. Serot, Nucl. Phys. A606, 508 (1996)
5. **sly**: F. Douchin and P. Haensel, Astron. Astrophys. 380, 151 (2001)
6. **pal6**: M. Prakash, T. L. Ainsworth, and Rev. Lett. 61, 2518 (1988)
7. **sqm1**: Prakash, M., Cooke, J. R., and Lattimer, J. M. 1995, Phys. Rev., D52, 661

The data sets were downloaded from the site:
http://xtreme.as.arizona.edu/NeutronStars/index.php/dense-matter-eos/
maintained by the Xtreme Astrophysics Group at the University of Arizona.

3

Results and discussion

3.1 A simple example - degenerate ideal neutron gas

We will use the example of the ideal gas EoS used by Oppenheimer and Volkoff to illustrate some of the broad themes that we come across in the study of neutron star models.

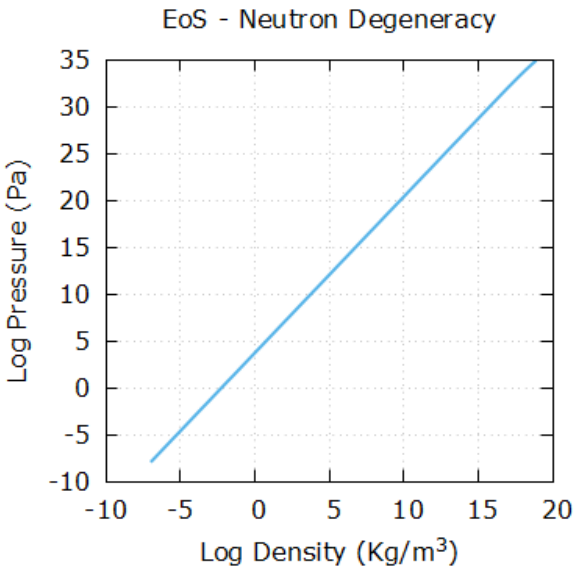

Figure 3.1: Equation of state - Ideal gas

The graph of log P vs log ρ is a straight line of slope $\simeq 1.665$. This is almost equal to $\frac{5}{3}$, the adiabatic index corresponding to a non relativistic ideal gas at 0 K. Thus, for most of the density range, the neutron gas remains non relativistic. Whereas a gas of degenerate electrons becomes relativistic at $\sim 10^{10} kg\, m^{-3}$, since it is much lighter than neutrons.

The mass radius relation corresponding to this EoS is given below (Fig 3.2a). We can see that as mass increases, radius decreases. In order to support a larger mass, the pressure and hence the density has to be greater. The mass of the neutron star does not increase

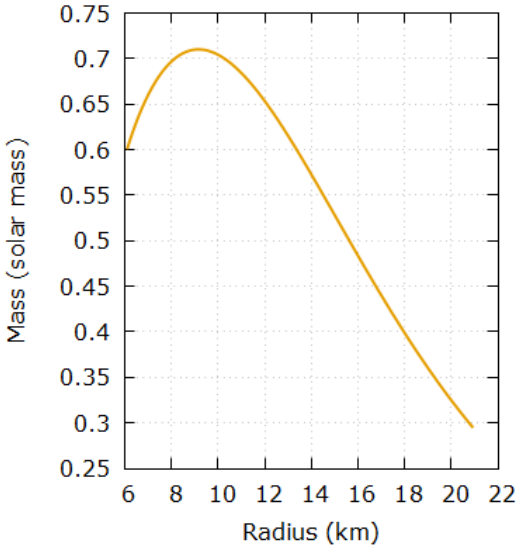

(a) Mass-Radius relation - Ideal gas

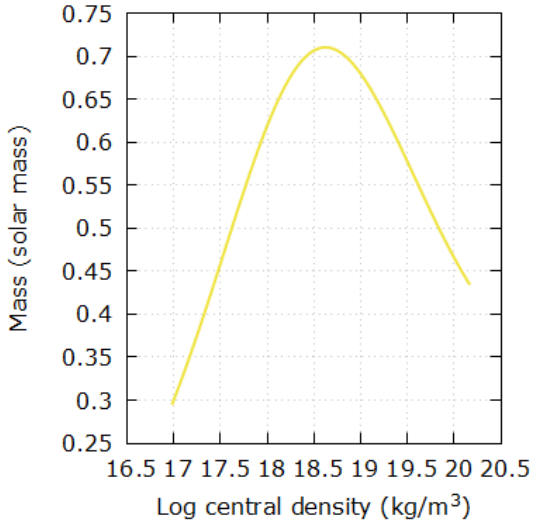

(b) Mass vs central density - Ideal gas

indefinitely, but there is a maximum mass beyond which for decreasing radius, mass also decreases. The value of the maximum mass of a neutron star as predicted by this model is approx 0.71 solar masses at a radius of about 9.18 km.

The maximum mass corresponds to a log central density of $\simeq 18.5$ (Fig 3.2b) Any further increase in central density results in the mass decreasing corresponding to the branch of the M-R plot beyond the maximum mass. It can be shown that neutron stars on this branch are unstable.

Figure 3.3a shows the variation of density within a neutron star for different masses. A common feature that can be observed is that density does not change much until the radius becomes equal to the radius of the star, after which there is a steep drop. The steep drop is a signature of a solid surface. We know that neutron stars must have solid surfaces to be able to anchor magnetic fields and produce stable pulsars. But it is very interesting to see that the pure neutron Fermi gas EoS, which contains no information about solid state of matter, reproduces the expected result.

The density profile is steeper for higher mass stars than lower mass ones. The physical interpretation of the equation of hydrostatic equilibrium (in this case, the TOV Eq 1.7) is that the inward gravitational force on an slab of mass with unit area and infinitesimal height within a star is balanced by the pressure gradient at that point. If the mass within this slab increases, then in order to support it against gravity, the pressure gradient and hence the density gradient has to be greater.

Though the density profile for the M = 0.33 solar mass star looks flat for most of the star's interior, the moment of inertia is about half of what it should have been ($2/5MR^2$) if the star had uniform density throughout (See Fig 3.3b). This is because the density decreases by a couple of orders of magnitude *close to the surface*. The decrease occurs over a small part of the star, but it has a greater effect on the MoI since it happens at a larger radius.

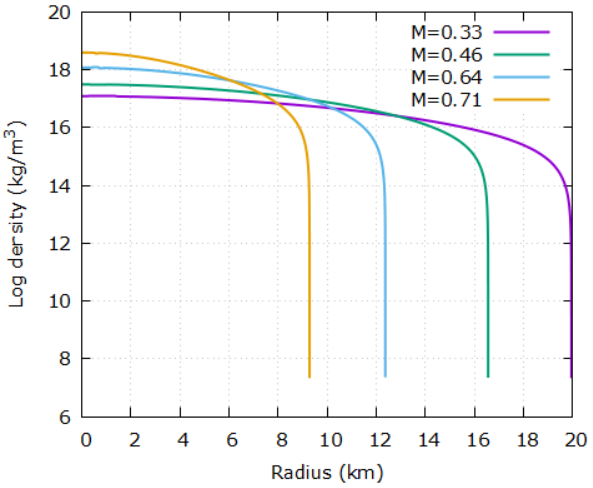

(a) Density profile - Ideal gas

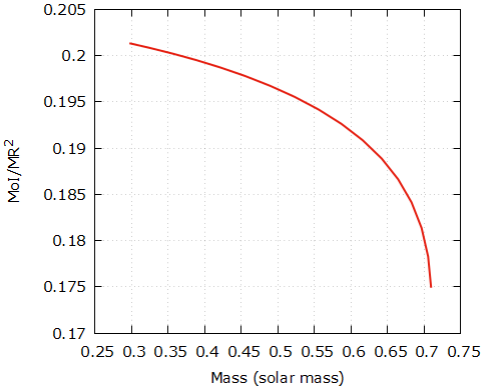

(b) MoI vs Mass - Ideal gas

As mass increases, density profile becomes steeper, and the moment of inertia reduces further.

For our final exercise, we will compare the mass radius relation when Newtonian gravity is used instead of GR, with the one predicted using GR.

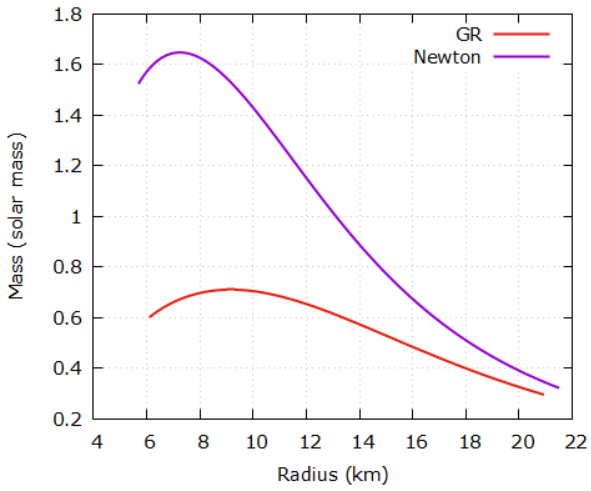

Figure 3.4: Newton vs GR - Ideal gas

As can be seen in Fig 3.4, Newtonian gravity predicts a much greater maximum mass and a larger radius for a given mass as compared to GR. Thus, for dense objects such as neutron stars, there is a significant deviation of GR from Newtonian gravity. Neutron stars can act as probes to test General Relativity's predictions!

The maximum mass predicted by this model, 0.71 solar masses, is far lesser than the Chandrasekhar limiting mass for white dwarfs which is 1.4 solar masses. All neutron stars born in supernovae are expected to be more massive than 1.4 solar masses and indeed most neutron star masses measured today are greater than this. Thus, the ideal gas equation of state is clearly incorrect.

3.2 Realistic Equations of state - AP3

Now that we have understood the basic features of neutron star models, we can explore some of the subtleties found in realistic equations of state.

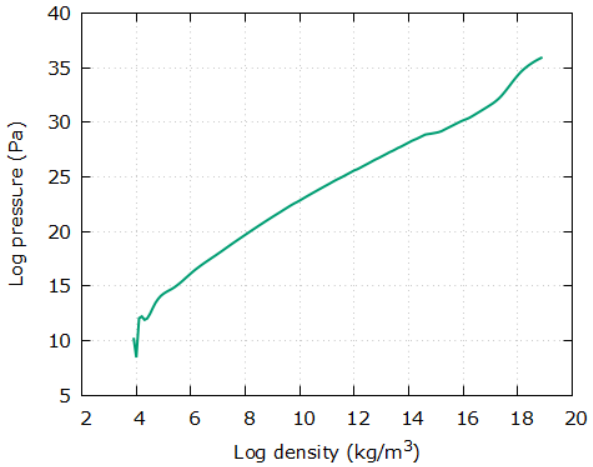

Figure 3.5: Equation of state - AP3

From the plot of log P vs log ρ (Fig 3.5), we can identify the three regimes described in section 1.5. Below neutron drip - which corresponds to a log density of $\simeq 14.6$ according to BPS, the slope of the graph is approximately equal to $\frac{4}{3}$. This is because all the pressure in this regime is due to relativistically degenerate electrons as described before. At neutron drip, the BPS equation of state is smoothly matched to the BBP EoS. The slope of the graph reduces sharply at this point due to the appearance of neutrons. Nuclear saturation occurs at a log density of about 17.4. AP3 refers to the nuclear equation of state above saturation density.

The equation of state is much stiffer just above saturation density than anywhere else in the graph. This is because AP3 has assumed a repulsive nuclear potential at distances comparable to the size of a nucleus. Hence, at these densities, the nuclear matter strongly resists squeezing leading to a steep slope.

The mass radius relation and mass vs central density plots can be found in figures 3.6a and 3.6b. As before, these plots show a maximum. The maximum mass of a stable neutron star in this EoS is **2.39 solar masses** with a radius of **10.78 km** and log central density of **18.37** (in kg/m^3 units).

As mass increases, radius decreases until a mass of around 0.5 solar masses. For further increase in mass beyond this point, the radius is almost a constant (increases slightly) until it reduces again close to the maximum mass. This can be explained as follows. The log central density corresponding to 0.5 solar masses is $\simeq 17.7$. For stars more massive than 0.5 solar masses, most of their interior is above the nuclear saturation density (17.4). The stiff nuclear equation of state resists compression when more mass is added to the star. As mass increases, so does the fraction of the star's interior with density above ρ_{nuc}. The net

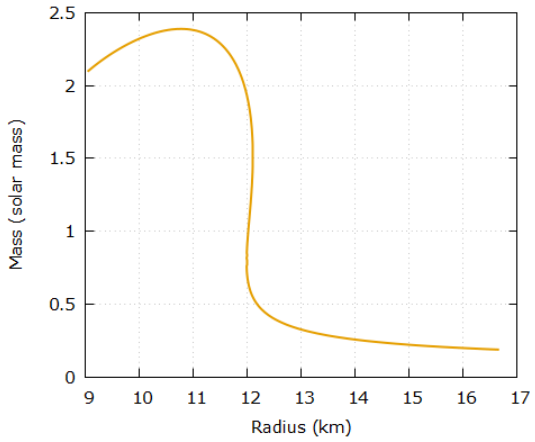

(a) Mass-Radius relation - AP3

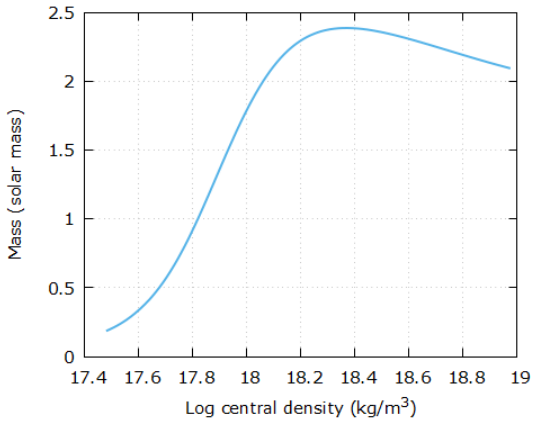

(b) Mass vs central density - AP3

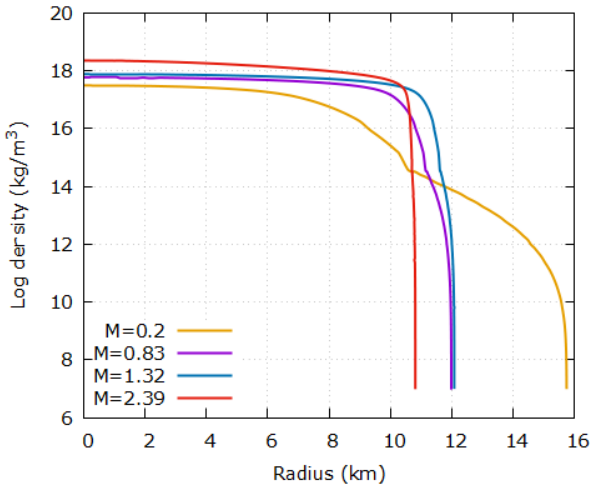

(c) Density profile - AP3

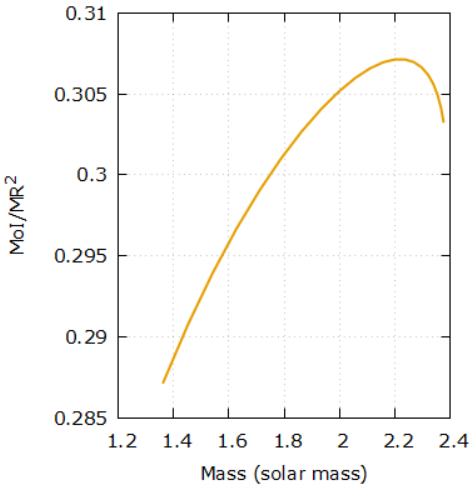

(d) MoI vs Mass - AP3

effect of addition of mass when the initial mass is greater than 0.5 solar masses, seems to be a slightly greater increase in outward pressure than inward gravitational pull, leading to the new equilibrium radius being slightly larger than the initial radius. Whereas in lower mass stars, most of the interior is below saturation density and the EoS is softer than even the pure neutron degeneracy pressure (Sec 3.1). Therefore, radius decreases rapidly with increasing mass in this regime.

We can better understand what is happening if we look at the density plots (Fig 3.6c). For M = 0.2 solar masses, nearly three quarters of the star is below saturation density. For M = 1.32 solar masses, nearly all of the star's interior is above saturation density. As mass increases, the density profiles are becoming flatter (as opposed to the pure neutron degeneracy case). This is again because the stiff equation of state above ρ_{nuc} is able to produce enough pressure to support the star, with smaller density gradients. As a direct consequence of this, the moment of inertia of larger mass stars are closer to their uniform density values than smaller mass stars (Fig 3.6d).

The range of MoI/MR^2 for masses above 1.4 solar masses is about 0.02. Hence, the ex-

pression for moment of inertia is roughly the same for all observed neutron stars in this EoS.

Finally, Fig 3.7 shows the mass radius relation if Newtonian gravity was used instead of GR. Due to the weaker gravitational force in Newton's gravity, radius increases drastically after saturation density is reached in the star's interior. Unlike the pure neutron degeneracy case, this plot is qualitatively also very different from the GR case and it predicts a maximum mass nearly 20 times the mass predicted by using GR.

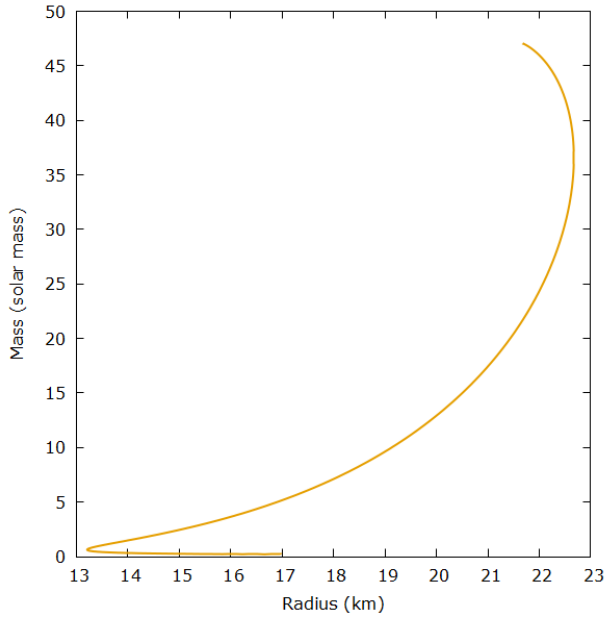

Figure 3.7: AP3 mass-radius relation - Newtonian

The qualitative features of all the other equations of state considered in this project are the same as ap3 and hence for the rest of the equations of state I will only be calculating the mass radius relation and moment of inertia.

3.3 Comparing Equations of state

All realistic equations of state (except sqm1) only differ in the regime above nuclear saturation density (Fig 3.8). Mass radius relations has been plotted in Fig 3.9a.
SQM is an EoS describing strange stars composed entirely of quark matter. The mass radius relation and EoS of sqm is qualitatively very different from the rest. Due to the very stiff EoS at lower densities in sqm, as mass increases, so does radius. These quark stars will not have a solid surface.

Fig 3.9b shows moment of inertia vs mass for all the equations of state for masses above 1.4 solar masses. Again, MoI/MR^2 does not vary much, even across equations of state, in this range given the precision of all quantities we are dealing with.
Finally in Fig 3.10 below, the observed masses of three of the most massive neutron stars known, whose masses have been measured with a reliable degree of precision, have been

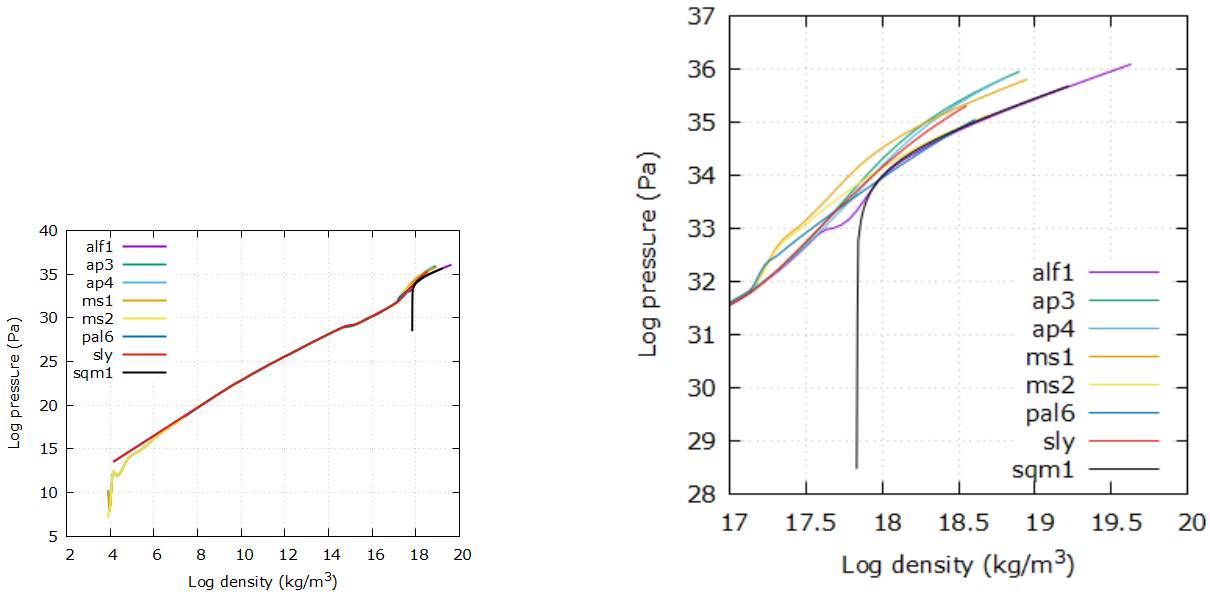

Figure 3.8: Comparison of equations of state

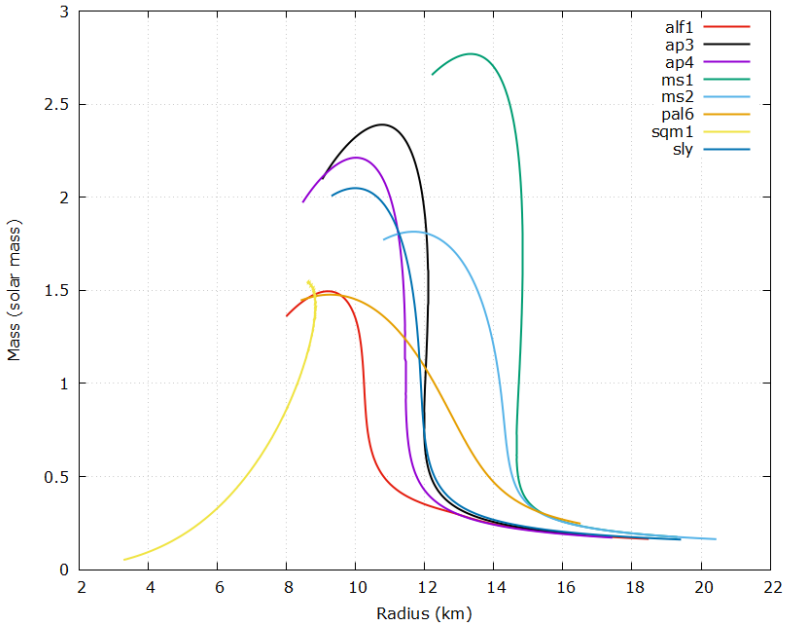

(a) Comparison of mass radius relations

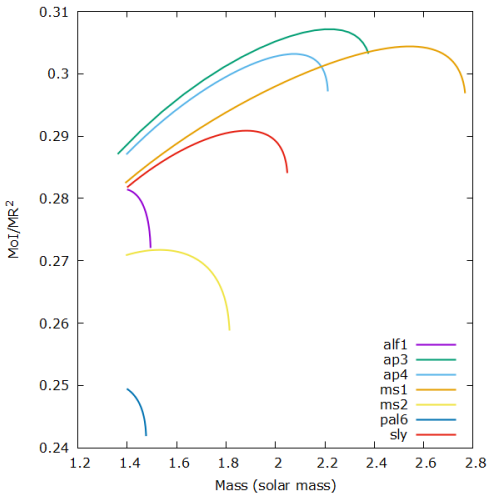

(b) Comparison of moment of inertia

plotted. The solid lines correspond to the mean values of the observed masses and the dotted lines correspond to the mean error in the measured values. All three neutron stars are in binary systems with white dwarf companions. The mass of such neutron stars is inferred by carefully measuring the time delay between the arrival of successive pulses as the pulsar moves through its orbit and accounting for that delay. The pulsars plotted here are PSR J1614-2230 with a mass of 1.908 $\pm$ 0.016 [2] solar masses, PSR J0348+0432 with a mass of 2.01 $\pm$ 0.04 [1] solar masses, and PSR J0740+6620 with a mass of 2.08 $\pm$ 0.07 [4] solar masses.

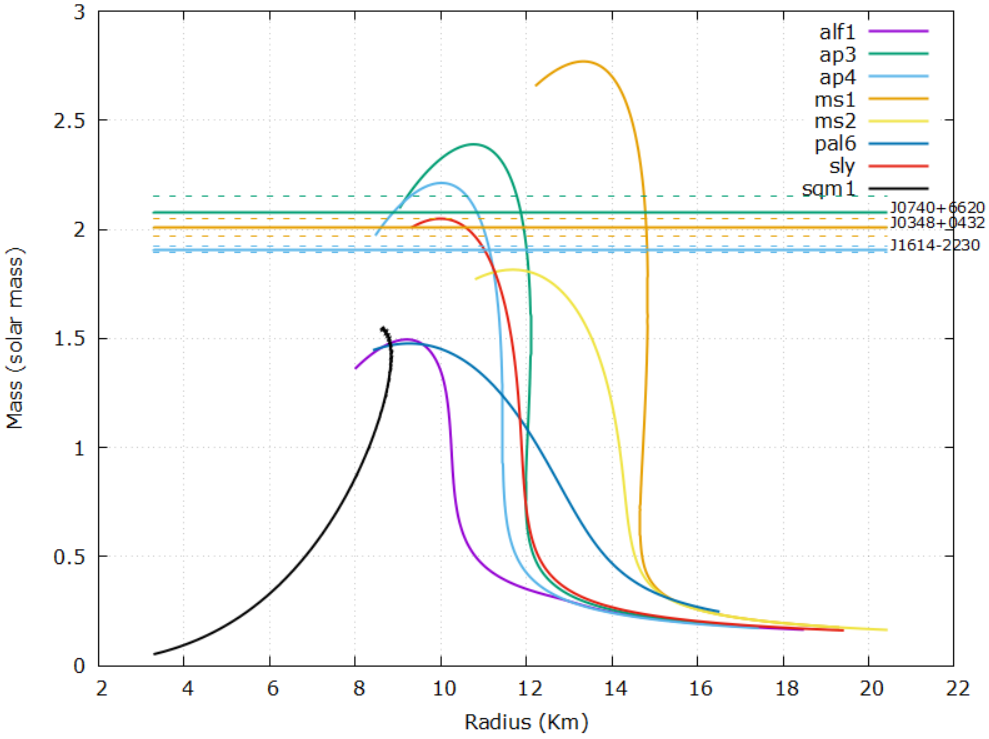

Figure 3.10: Observed masses of neutron stars

3.4 Conclusion

In this project, we have used several proposed equations of state and have numerically calculated the corresponding mass-radius relations, moment of inertia and density profiles. We then plotted the heaviest known neutron stars on the M-R plots (fig 3.10).

The M-R plots of ms2, pal6, alf1 and sqm1 equations of state lie completely below the lowest possible mass of this data set. Hence, these EoS's are unlikely to be the correct description of the interior of a neutron star. On the other hand, the equations of state ap3, ap4, and ms1 predict a maximum mass greater than the highest possible mass in this data set.

As more observations of neutron stars are made, we can better constrain the dense matter equation of state and thus hope to understand the nature of the exotic forms of matter that can exist at such high densities.

Bibliography

[1] J. Antoniadis et al. "A Massive Pulsar in a Compact Relativistic Binary". In: *Science* 340.6131 (Apr. 2013), pp. 1233232–1233232. ISSN: 1095-9203. DOI: 10.1126/science.1233232. URL: http://dx.doi.org/10.1126/science.1233232.

[2] Zaven Arzoumanian et al. "The NANOGrav 11-year Data Set: High-precision Timing of 45 Millisecond Pulsars". In: 235.2 (Apr. 2018), p. 37. DOI: 10.3847/1538-4365/aab5b0. URL: https://doi.org/10.3847/1538-4365/aab5b0.

[3] "Cold Equation of State Below Neutron Drip". In: *Black Holes, White Dwarfs, and Neutron Stars*. John Wiley Sons, Ltd, 1983. Chap. 2, pp. 17–54. ISBN: 9783527617661. DOI: https://doi.org/10.1002/9783527617661.ch2. eprint: https://onlinelibrary.wiley.com/doi/pdf/10.1002/9783527617661.ch2. URL: https://onlinelibrary.wiley.com/doi/abs/10.1002/9783527617661.ch2.

[4] E. Fonseca et al. "Refined Mass and Geometric Measurements of the High-mass PSR J0740+6620". In: *The Astrophysical Journal Letters* 915.1 (July 2021), p. L12. ISSN: 2041-8213. DOI: 10.3847/2041-8213/ac03b8. URL: http://dx.doi.org/10.3847/2041-8213/ac03b8.

[5] J. R. Oppenheimer and G. M. Volkoff. "On Massive Neutron Cores". In: *Phys. Rev.* 55 (4 Feb. 1939), pp. 374–381. DOI: 10.1103/PhysRev.55.374. URL: https://link.aps.org/doi/10.1103/PhysRev.55.374.

[6] Feryal Özel and Paulo Freire. "Masses, Radii, and the Equation of State of Neutron Stars". In: *Annual Review of Astronomy and Astrophysics* 54.1 (2016), pp. 401–440. DOI: 10.1146/annurev-astro-081915-023322. eprint: https://doi.org/10.1146/annurev-astro-081915-023322. URL: https://doi.org/10.1146/annurev-astro-081915-023322.

[7] William H. Press et al. *Numerical Recipes 3rd Edition: The Art of Scientific Computing*. 3rd ed. Cambridge University Press, Sept. 2007. ISBN: 0521880688. URL: http://www.amazon.com/exec/obidos/redirect?tag=citeulike07-20%5C&path=ASIN/0521880688.